Jetting to dripping in compound liquid jets falling under gravity

Afzaal, Muhammad F.; Uddin, Jamal

DOI:
10.1063/5.0168339

Document Version
Publisher's PDF, also known as Version of record

Citation for published version (Harvard):
Afzaal, MF & Uddin, J 2023, 'Jetting to dripping in compound liquid jets falling under gravity', *Physics of Fluids*, vol. 35, no. 9, 094119. https://doi.org/10.1063/5.0168339

Physics of Fluids

RESEARCH ARTICLE | SEPTEMBER 21 2023

Jetting to dripping in compound liquid jets falling under gravity

Muhammad F. Afzaal ; Jamal Uddin

Physics of Fluids 35, 094119 (2023)
https://doi.org/10.1063/5.0168339

Physics of Fluids ARTICLE pubs.aip.org/aip/pof

Jetting to dripping in compound liquid jets falling under gravity

Cite as: Phys. Fluids **35**, 094119 (2023); doi: 10.1063/5.0168339
Submitted: 18 July 2023 · Accepted: 4 September 2023 ·
Published Online: 21 September 2023

Muhammad F. Afzaal[1] and Jamal Uddin[2,a)]

AFFILIATIONS

[1]Division of Physical Sciences and Engineering, King Abdullah University of Science and Technology, Thuwal 23955-6900, Saudi Arabia
[2]School of Mathematics, University of Birmingham, Edgbaston, Birmingham B15 2TT, United Kingdom

[a)]Author to whom correspondence should be addressed: J.Uddin@bham.ac.uk

ABSTRACT

In recent years, there has been a substantial growth in technologies, which exploits the disintegration of a compound thread of fluid to produce compound droplets or capsules. In many cases, careful control of the relevant operating and material parameters can determine a range of features, including capsule sizes, production rates, and wastage. In this paper, we investigate the transition between jetting and dripping of a compound inviscid liquid jet falling under gravity in a surrounding gas. We derive an analytical expression for the dispersion relation, which takes into account the non-uniform nature of the jet, which we then solve numerically utilizing the cusp map method and its significant reduction in computational effort required in identifying saddle points of the dispersion relation. Particular attention is paid to investigating the effects of the inner-to-outer surface tension ratio σ and initial jet radii, χ, as well as the influence of gravity on critical Weber numbers, We_c (which mark the transition between jetting and dripping). Our results provide the convective to absolute instability boundary for a number of different parameter values.

I. INTRODUCTION

A simple literature search on the topic of the instability of a thread of fluid will provide a glimpse of the historical as well as modern, widespread interest in this subject area. Moreover, it will highlight that this has been a topic of interest stretching back to the early classical works of Rayleigh[1] and Savart[2] in the late nineteenth century, and that it continues to focus the minds of researchers well into the present. These authors considered a single thread (or jet) of fluid disintegrating due to growing capillary instabilities on the free surface. Since then, a large body of literature has accumulated investigating myriad different settings, applications, and aspects of this prototypical setup considered by Rayleigh. A testament to the growing importance of liquid jet rupture can be gauged by the number of reviews in modern times, including those of Lin,[3] Eggers,[4] Eggers and Villermaux,[5] and, more recently, that of Montanero and Ganan-Calvo.[6]

One recent industrial application has been the use of fluid threads in the production of encapsulated droplets. In particular, encapsulation of biologically active substances, like cells or proteins, is a growing field of biomedical research (Jayaprakash and Sen[7]). Advances in this field are unlocking the potential for refined treatment of many diseases, including cancer and diabetes (Liu *et al.*[8]). Cell encapsulation involves encasing cells in a protective outer membrane and forms a fundamental part of modern day medical and pharmaceutical research. Encapsulated cells, which belong to a wider class of biocapsules, offer a promising route in avoiding hostile *in vivo* responses of the bodies' natural immune system. Mechanical manufacturing of capsules is varied but generally relies on some form of dripping or liquid jet breakup (Mishra[9]). Coaxial jet atomization (where a concentric nozzle is used to produce a compound liquid jet) provides a simple and efficient means to generate capsules, whereby the controlled breakup process between the inner and outer liquid jets can be used to generate tailor made capsules.

While the breakup of compound liquid jets is inherently more complicated than its single jet counterpart, it, nevertheless, relies on similar fundamental principles. The first works regarding compound liquid jets were experimental in nature and those developed by Hertz and Hermanrud[10] whose pioneering works demonstrated the viability of producing compound liquid drops (or capsules) from the breakup of a compound liquid jet. The same authors identified three types of instabilities based on a combination of parameter values (including surface tension ratio, jet radii, jet velocity, and density ratios).

Sanz and Meseguer[11] were the first to perform a theoretical stability analysis of a compound jet using an inviscid fluid model to identify two modes of instability. These modes were associated with capillary forces on the inner and outer interfaces of the compound jet and were unstable if waves were longer than the inner (called the *squeezing mode* or *sinuous mode*) and outer circumference (called the *stretching mode* or *para-sinuous mode*) of the compound jet, respectively. Radev and Tchavdarov[12] and Shkadov and Sisoev[13] derived a linear model from the two-dimensional equations of motion, numerically solved the resulting eigenvalue problem, and were then able to identify qualitative conditions for specific breakup points of the compound jet. Chauhan *et al.*[14] considered the temporal instability of a compound liquid jet, paying particular attention into growth rates and amplitude ratios of the stretching mode so as to better understand the specific nature of breakup and whether the inner (or core) fluid breaks first and, thus, promotes the formation of compound droplets. These ideas were extended by Qiao *et al.*[15] to explore temporal instability of viscous compound jets with a radial thermal field. They determined that the para-sinuous mode is susceptible to instability with changes in the thermal conductivity and specific heat capacity. The nonlinear dynamics of compound liquid jets have been considered by Uddin and Decent[16] who investigated droplet formation using a finite difference scheme to solve the one-dimensional nonlinear governing equations. The effects of viscosity were considered by Ruo *et al.*[17] and Suryo *et al.*[18] These authors used a Galerkin/finite element method to numerically determine the conditions for compound jet formation.

Liquid jets that are accelerating due to, for example, rotational or gravitational forces have received less attention. Recently, Amini *et al.*[19] investigated the effects of gravitational forces on a liquid jet, concluding that gravitational forces can alter maximal growth rates toward shorter waves and increase cutoff frequencies. Vu *et al.*[20,21] have investigated the unsteady evolution of compound jet interfaces numerically using the front-tracking/finite difference method. Their results provide good agreement with experimental results but do not take into account three-dimensional effects and most notably the presence of nonaxisymmetric distortions to the jet. Mohsin *et al.*[22] investigated the temporal instability of a compound jet falling under gravity with Afzaal[23] and Afzaal *et al.*,[24] considering temporal and spatial instabilities for compound jets falling under gravity. Afzaal and Uddin[25] considered the effects of the surrounding medium (typically taken as a gas) and nonaxisymmetric disturbances.

Keller *et al.*[26] were the first to consider spatial instability in liquid jets, and they demonstrated that, for very large Weber numbers, temporal and spatial disturbances are analytically related. However, it was not until Leib and Goldstein[27] that absolute instability of an inviscid liquid jet was first identified, and in Leib and Goldstein,[28] they were able to determine the critical Weber number, as a function of the Reynolds number, for which a liquid jet would be either convectively unstable (jetting) or absolutely unstable (dripping). An excellent review of the topic of dripping and jetting in liquid jets was provided by Montanero and Gana-Calvo,[6] where it is stated that the distinction between the two types of instabilities is not always clear. Lin and Lian[29] considered the effects of the surrounding gas on the absolute instability of a liquid jet. Chauhan *et al.*[30] have considered the absolute instability of an inviscid compound liquid jet as has Vadivukkarasan[31] who identified critical Weber numbers based on various parameters of the compound liquid jet.

The breakup mode of a fluid thread can be predicted via the transition between convective-to-absolute instability (see Montanero and Gana-Calvo[6]). This has been demonstrated in a number of cases,[3] although it should be noted that other instability mechanisms may also lead to a transition between jetting and dripping. The transition from convective to absolute instability is characterized, typically, by the difference in location of droplet formation. In the case of jetting, droplets are formed some distance downstream of the nozzle (leading to the appearance of a column or jet of fluid before formation of droplets). In the case of dripping, droplets form in the immediate vicinity of the nozzle.[32] A better understanding of this transition is useful in many industrial applications, including recent attempts to control satellite droplets using a drainage device.[33]

In this paper, we examine the absolute instability of a compound inviscid liquid jet, which is falling vertically under the influence of gravity in the presence of a surrounding gas. We pay particular attention to the transition from convective to absolute instability for a range of parameter values and identify the critical Weber numbers involved. Our results provide a systematic approach, using the cusp map method of Kupfer, Bers, and Ram,[34] to understanding the theoretical transition between dripping and jetting in a compound liquid jet falling under gravity.

II. PROBLEM FORMULATION

In this section and the next section, we briefly reformulate the problem presented in Afzaal *et al.*[24] We begin by considering an inviscid compound jet, which emerges from a concentric tube with exit velocity U and moves in a surrounding gas (which is initially stationary). The initial outer radius of the compound jet is a with the inner jet having a smaller initial radius χa, where $0 < \chi < 1$. It is assumed that the compound jet, after emerging from a circular orifice, falls in a vertical direction under the influence of gravity. It is also assumed that all the fluids are incompressible and immiscible. The geometry of the compound jet is described in a cylindrical coordinate system (r, θ, x), where r is the radial component, θ is the azimuthal component, and x represents the axial direction of the jet (see Fig. 1). The velocity vector

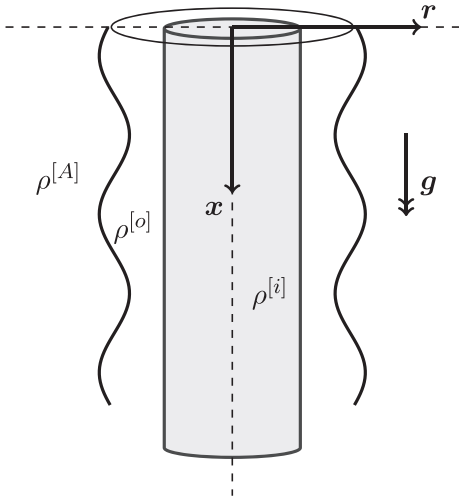

FIG. 1. A schematic of the compound jet depicting the inner and outer jets with some of the parameters. The inner and outer interfaces are given by $x = R(x, t)$ and $x = S(x, t)$, respectively, with the interfacial/surface tensions of the inner and outer interfaces given by $\sigma^{[i]}$ and $\sigma^{[o]}$.

describing the axisymmetric flow can be written as $\mathbf{u}^{[z]} = (v^{[z]}, 0, u^{[z]})$, where the subscript $z = I$ is for the inner fluid, $z = O$ is for the outer fluid, and $z = A$ is for the surrounding gas. Here, we denote $r = R(x,t)$ as the interface of inner fluid with the outer one, $r = S(x,t)$ as the interface of outer fluid with the surrounding gas, $\sigma^{[I]}$ is the interfacial tension at the interface $r = R(x,t)$, and $\sigma^{[O]}$ is the surface tension at the interface $r = S(x,t)$. The density of the fluids is denoted by $\rho^{[z]}$, and the pressure and the time are denoted as $p^{[z]}$ and t, respectively. The vector representing the acceleration due to gravity is taken as $\mathbf{g} = (0,0,g)$. In addition, $\sigma^{[I]}$ and $\sigma^{[O]}$ are assumed to be constant at the inner and the outer interface, respectively.

The continuity equation and Euler's equation, which describe the resulting dynamics of the compound jet, are given by

$$\frac{\partial u^{[z]}}{\partial x} + \frac{\partial w^{[z]}}{\partial r} + \frac{v^{[z]}}{r} = 0, \tag{1}$$

$$\frac{\partial u^{[z]}}{\partial t} + u^{[z]}\frac{\partial u^{[z]}}{\partial x} + v^{[z]}\frac{\partial u^{[z]}}{\partial r} = -\frac{1}{\rho^{[z]}}\frac{\partial p^{[z]}}{\partial x} + (\delta_{\mathbf{Iz}} + \delta_{\mathbf{Oz}})g, \tag{2}$$

and

$$\frac{\partial v^{[z]}}{\partial t} + u^{[z]}\frac{\partial v^{[z]}}{\partial x} + v^{[z]}\frac{\partial v^{[z]}}{\partial r} = -\frac{1}{\rho^{[z]}}\frac{\partial p^{[z]}}{\partial r}, \tag{3}$$

where $\delta_{\mathbf{Iz}}$ and $\delta_{\mathbf{Oz}}$ are the Kronecker delta symbols with free index z. These equations are supplemented by the kinematic conditions and the normal stress conditions on the interfaces. The kinematic conditions, at the interface $r = R(x,t)$, are given by

$$w^{[z]} = \frac{\partial R}{\partial t} + u^{[z]}\frac{\partial R}{\partial x}, \tag{4}$$

where $z = I, O$. Similarly, the kinematic conditions, at the interface $r = S(x,t)$, are given by

$$w^{[z]} = \frac{\partial S}{\partial t} + u^{[z]}\frac{\partial S}{\partial x}, \tag{5}$$

where $z = O, A$. For inviscid fluids, we have the classical free surface condition of constant pressure and hence zero tangential stress condition. The normal stress conditions, at the interfaces $r = R(x,t)$ and $r = S(x,t)$, are

$$p^{[I]} - p^{[O]} = \sigma^{[I]}\kappa^{[I]}, \qquad p^{[O]} - p^{[A]} = \sigma^{[O]}\kappa^{[O]}, \tag{6}$$

respectively, where $\kappa^{[I]}$ is the mean curvature of the inner free surface and $\kappa^{[O]}$ is the mean curvature of the outer free surface, which are given by

$$\kappa^{[I]} = \frac{\partial}{\partial x}\left(-\frac{1}{E^{[I]}}\frac{\partial R}{\partial x}\right) + \frac{\partial}{\partial r}\left(\frac{r}{E^{[I]}}\right), \tag{7}$$

$$\kappa^{[O]} = \frac{\partial}{\partial x}\left(-\frac{1}{E^{[O]}}\frac{\partial S}{\partial x}\right) + \frac{\partial}{\partial r}\left(\frac{r}{E^{[O]}}\right), \tag{8}$$

where

$$E^{[I]} = \left(1 + \left(\frac{\partial R}{\partial x}\right)^2\right)^{\frac{1}{2}}, \quad E^{[O]} = \left(1 + \left(\frac{\partial S}{\partial x}\right)^2\right)^{\frac{1}{2}}. \tag{9}$$

We can non-dimensionalize the velocity components with the initial jet velocity U at the tube exit, so we have $\bar{v}^{[z]} = v^{[z]}/U$ and $\bar{u}^{[z]} = u^{[z]}/U$, radial lengths with the outer jet radius a, so that $\bar{r} = r/a$ and the axial length with a characteristic wavelength L (typically much greater than a) in the axial direction as $\bar{x} = x/L$. The time and the pressure are scaled by $\bar{t} = tU/L$ and $\bar{p}^{[z]} = p^{[z]}/\rho^{[O]}U^2$, respectively. By assuming the jet is slender, we define a small parameter ϵ as $\epsilon = a/L \ll 1$. The dimensionless forms of the inner and outer radii of the jet at the nozzle are $R(0,t) = \chi$ and $S(0,t) = 1$, respectively. The resulting set of equations contain two key non-dimensional numbers, namely, the Weber number $We = \rho^{[O]}U^2a/\sigma^{[I]}$, which measures the ratio of surface tension forces to inertia, and the Froude number $Fr = gL/U^2$, which measures the relative importance of gravity forces over inertia.

III. STEADY STATE SOLUTIONS

In order to find the steady state solutions, we consider a quiescent gas so that $\mathbf{u}^{[\mathbf{A}]} = (0,0,0)$. We expand our variables (after dropping the overbars) using an asymptotic expansion, so that we have

$$\left[u^{[z]}, w^{[z]}, p^{[z]}\right](r,x,t) = \left[(\delta_{Iz} + \delta_{IO})u_0^{[z]}(x), 0, p_0^{[z]}(x)\right] + \epsilon\left[\hat{u}^{[z]}(r), \hat{w}^{[z]}(r), \hat{p}^{[z]}(r)\right], \tag{10}$$

$$[R,S](x,t) = [R_0(x), S_0(x)] + \epsilon[R_1(x,t), S_1(x,t)]. \tag{11}$$

Upon substitution of this expansion into (6)–(9), we obtain the following expressions for the inner and outer pressures:

$$p^{[O]}(x) = \frac{1}{We(S_0(x))}, \quad p^{[I]}(x) = \frac{1}{We}\left(\frac{\sigma}{R_0(x)} + \frac{1}{S_0(x)}\right). \tag{12}$$

The remaining equations then lead to the following set of equations:

$$u^{[I]}\frac{\partial u^{[I]}}{\partial x} = -\frac{1}{\rho We}\frac{\partial}{\partial x}\left(\frac{\sigma}{R_0(x)} + \frac{1}{S_0(x)}\right) + \frac{1}{Fr^2}, \tag{13}$$

$$u^{[O]}\frac{\partial u^{[O]}}{\partial x} = -\frac{1}{We}\frac{\partial}{\partial x}\left(\frac{1}{S_0(x)}\right) + \frac{1}{Fr^2}, \tag{14}$$

where $\rho = \rho^{[I]}/\rho^{[O]}$ and $\sigma = \sigma^{[I]}/\sigma^{[O]}$ are the density and surface tension ratios between the inner and outer fluid, respectively. Moreover, we make use of the symbol ρ^G to represent the density ratio between the density of the surrounding gas and the outer liquid density. Using (12)–(14) and making use of (1), (4), and (5) and with appropriate conditions at $x = 0$, we can solve for $u_0^{[O]}(x)$ and $u_0^{[I]}(x)$. More details as well as solutions for various parameter values can be found in Afzaal *et al.*[24] and Afzaal and Uddin.[25]

IV. LINEAR ANALYSIS

We now consider a linear temporal instability analysis of an axisymmetric compound liquid jet moving in a surrounding gas. To this end, we consider small perturbations to the steady state solutions found in Sec. III. We note that the evolution of the jet depends on a length scale $x = O(1)$, but disturbances along the jet are typically much smaller and are comparable to ϵ when $x = O(1)$. In other words, we can say that the disturbances are typically of the order of jet radius a. We, therefore, consider traveling short waves of the form $e^{\omega\bar{t} + ik\bar{x}}$, where $k = k(x) = O(1)$ and $\omega = \omega(x) = O(1)$ are the frequency and

wavenumber of disturbances, respectively. Additionally, $\bar{x} = x/\epsilon$ and $\bar{t} = t/\epsilon$ are small length and time scales, respectively. Thus, we have a multiple scale formulation as the perturbations grow along the jet having wavelength of $O(\epsilon)$. Now we introduce small time dependent perturbations to the steady state solutions, which take the following form:

$$(u^{[z]}, 0, v^{[z]}) = (\delta_{\mathbf{Iz}} + \delta_{\mathbf{Oz}})(u_0^{[z]}, 0, v_0^{[z]}) + \Lambda(\bar{u}^{[z]}(r), 0, \bar{v}^{[z]}(r))\Omega, \quad (15)$$

$$(p^{[z]}, R, S) = (p_0^{[z]}, R_0, S_0) + \Lambda(\bar{p}^{[z]}(r), \bar{R}, \bar{S})\Omega, \quad (16)$$

where $\Omega = \exp(\omega\bar{t} + ik\bar{x})$ and $0 < \Lambda \ll \epsilon$. Substituting the expansions (15) and (16) into the non-dimensionalized form of equations (1)–(12) yields a set of equations, which can be reduced to the dispersion relation,

$$D(\omega, k; We, \sigma, \rho, \rho^G, \chi, x) = 0, \quad (17)$$

where D is the determinant of the matrix

$$\begin{bmatrix}
\frac{1}{i}(I_0'(kR) & 0 & 0 & 0 & -\omega + iku^{[I]} & 0 \\
0 & \frac{1}{i}(I_0'(kR) & -\frac{1}{i}(K_0'(kR) & 0 & -\omega + iku^{[O]} & 0 \\
0 & \frac{1}{i}(I_0'(kS) & -\frac{1}{i}(K_0'(kS) & 0 & 0 & -\omega + iku^{[O]} \\
0 & 0 & 0 & \frac{1}{i}(K_0'(kS) & 0 & -\omega \\
\frac{-\rho(\omega + iku^{[I]})}{ik} I_0(kR) & \frac{(\omega + iku^{[O]})}{ik} I_0(kR) & \frac{(\omega + iku^{[O]})}{ik} K_0(kR) & 0 & -\frac{\sigma}{We}\left(k^2 - \frac{1}{R^2}\right) & 0 \\
0 & \frac{-(\omega + iku^{[O]})}{ik} I_0(kS) & \frac{-(\omega + iku^{[O]})}{ik} K_0(kS) & \frac{\omega\rho^G}{ik} K_0(kS) & 0 & -\frac{1}{We}\left(k^2 - \frac{1}{S^2}\right)
\end{bmatrix}.$$

This has been fully derived in Afzaal *et al.*[24] (and in a more general form incorporating nonaxisymmetric flows in a previous publication Afzaal and Uddin[25]). We note that the aforementioned dispersion relation does not explicitly depend on the Froude number Fr, and instead, this dependency only enters via the steady state solutions $u_0^{[O]}$, $u_0^{[I]}$, R_0, and S_0 from Sec. III. In general, these will vary along jet axis x and will be different for different values of Fr.

We plot temporal growth rates in Fig. 2 for typical parameter values we use later on in Sec. V. In general, the dispersion relation, (17), produces four roots, of which typically two have positive growth rates and are, therefore, unstable. In temporal instability analysis, the wavenumber with the largest growth rate (that is $k = k^* = 0.564$ in Fig. 2) is termed the most unstable wavenumber. This wavenumber can then be used to predict the size of droplets (via determining the wavelength $\lambda = 2\pi/k$ associated with this most unstable wavenumber). In a compound liquid jet, there exist two types of growing modes: a stretching mode driven by disturbances larger than the circumference of the inner jet and a squeezing mode by wavelengths larger than the outer jet circumference. The behavior of these unstable modes has been shown to exhibit a variety of features under different parameter regimes (particularly when $\chi < 1/\sqrt{2}$ and for small σ).[11] In particular, there exist certain parameter regimes where the value of the most unstable wavenumber, k^*, may undergo a discontinuous transition[22] when a parameter (typically σ) is smoothly varied. This occurs because the temporal mode goes from having one local maxima (from which it is easy to identify k^*) to having two local maxima. This is described in more detail in Sanz and Meseguer[11] and Mohsin *et al.*[22] This theoretically predicted behavior has been exploited in Chauhan *et al.*[30] with a view to exploring parameter regimes where the distinction between convective and absolute instabilities will become, experimentally, easier to identify.

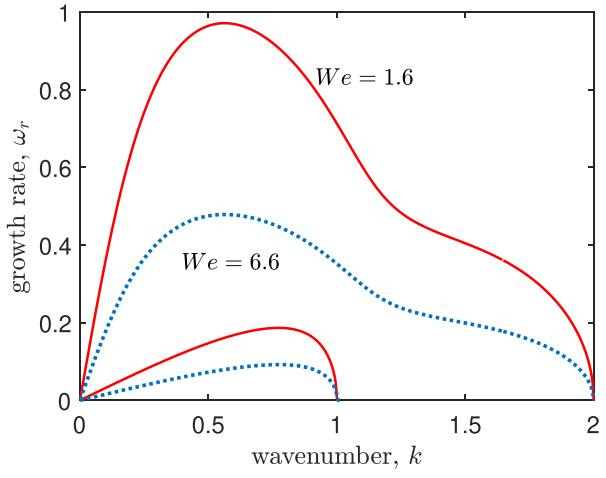

FIG. 2. A plot of the temporal growth rates, ω_r, for real values of the wavenumber, k, for the cases when $We = 1.6$ (continuous line) and $We = 6.6$ (dotted line) for the case where $\rho = 0.1$, $\rho^G = 0.001$, $\sigma = 0.1$, $x = 0$, and $\chi = 0.5$.

V. ABSOLUTE INSTABILITY ANALYSIS

Linear instability in liquid jets can be separated in two distinct groups: *convective instability* whereby disturbances grow in time but are convected downstream of the flow and *absolute instability* in which disturbances grow both upstream and downstream of the point of origin and subsequently dominate any region of the flow.[35] Determining the type of instability requires an understanding of the spatiotemporal behavior of the dispersion relationship. In general, it is sufficient to

determine the type of instability by analyzing the behavior of the Green's function,

$$G(x,t) = \int_L \frac{d\omega}{2\pi} \int_F \frac{dk}{2\pi} e^{(ikx+\omega t)} D^{-1}(k,\omega), \tag{18}$$

where L and F are Fourier and Laplace contours in the complex wavenumber and frequency plane, respectively, and $D(k,\omega)$ is the linear dispersion relation relating k with ω. In particular, one has convective instability when $G \to 0$ along the ray $x/t = 0$ [i.e., $G(x, t \to \infty) = 0$ for any finite x] with absolute instability when $G \to \infty$ for any fixed point x (see Charru[36]). In order to ensure convergence of the integral in (18), it is necessary, to avoid singularities of the dispersion relation, for appropriate deformations to the contour L. Evaluation of the aforementioned Fourier–Laplace integral is not always feasible (see Patne and Shankar[37]), and even in the case of large time solutions where analytical progress can be made, this involves deformation of the contour F, so that it passes through a saddle point, $k = k_0$, in the k-plane.[37] For absolute instability, it is necessary that disturbances have positive growth rate, $\omega_r > 0$,[38] and that the group velocity $\partial\omega/\partial k = 0$ at the saddle point k_0. Absolute instability will occur if the solution of the dispersion relation is a first-order saddle point in the complex k-plane (the saddle point occurring at some point in the plane, say k_0), which corresponds to a pinch point (also called a cusp point) in the complex ω-plane. A "cusp point" is defined as an intersection between mappings of $k(\omega)$ curves in the complex frequency plane. However, this is only a necessary condition and not a sufficient condition since the group velocity is zero at points other than at saddle points, including when two k-branches meet independently of whether the branches originated from the same half-k-plane or not. The aforementioned analysis requires an appreciation of the mapping between the complex frequency, ω, plane to the complex wavenumber, k, plane, and so it will involve solving $D(\omega,k) = 0$ to find k for a given ω.[43,44] In general, as is the case for our aforementioned dispersion relation, the function $D(\omega,k)$ is transcendental in k and, therefore, often numerically intensive to solve. A rather creative solution to avoid solving complex transcendental functions and utilizing the fact that in many cases, the dispersion relation is only a polynomial in ω (and therefore much more easily, and accurately, solved). Kupfer *et al.*[34] developed a mapping procedure (called the cusp map method), in which pinch points can be found by using mappings of selected contour lines from the complex k-plane into the complex ω-plane.

In particular, this method seeks to identify points in the complex ω plane, where the group velocity, $\partial\omega/\partial k$, is zero as well as whether these very points correspond to pinch points in the complex wavenumber plane. Solutions of $D(\omega,k) = 0$ and $\partial D(\omega,k)/\partial k = 0$ are branch points in the ω plane; for any point, $\omega = \omega_0$, which satisfies both these expressions, and for which $\partial^2 D(\omega_0,k_0)/\partial k^2 \neq 0$, then it can be shown that a local mapping $\omega - \omega_0 \sim (k - k_0)^2$ exists. Such a relationship signifies that a cusp will form in the complex frequency plane when a curve from the complex wavenumber plane (containing the point k_0) is mapped into the complex frequency plane.

The cusp map method, as developed by Kupfer *et al.*,[34] can be viewed as a systematic procedure to determine whether a cusp point corresponds to absolute instability or not. The primary feature of this method is a careful examination of the behavior of mappings of horizontal lines from the complex wavenumber plane [i.e., contours with fixed values of $Im(k) = k_i < 0$ and $0 < k_r < k_c$, where k_c is the cutoff wavenumber beyond which temporal modes are stable]. In order to find (any) cusp point, we must map such contour lines for different values of $k_i < 0$ and plot their images [via the dispersion relation $D(\omega,k) = 0$] in the complex ω-plane. In the case where $k_i = 0$, this leads to a reduced polynomial dispersion relation with real coefficients and may be solved via Ferrari's methods (e.g., see previous work in Mohsin *et al.*[22] and Afzaal and Uddin[25]). However, when $k_i < 0$, the resulting dispersion relation may not be solved using Ferrari's method, and instead, we resort to Muller's method to yield the numerical roots of the dispersion relation. As Muller's method requires a series of initial guesses, we complete a systematic search (through iterating between different initial guesses in the complex wavenumber plane such that $0 < k_r < k_c$ and $k_i < 0$) in order to determine the roots of the dispersion relation. The resulting images will form a series of contour lines in the complex ω-plane, of which one will form a cusp (if such a cusp point exists). This is demonstrated in Fig. 3 where a cusp can be seen to form when $k_i = -0.245$. In this same figure, we have shown the contours for the cases where k_i is slightly less and slightly more than this value (we chose $k_i = 0.23$ and $k_i = 0.26$ to make the differences between the contours clearer). The location in the frequency plane of this cusp point, denoted by $\omega = \omega_0$ [in Fig. 3 where we have that $\omega_0 = (0.043, -0.848)$], will be associated with a wavenumber $k = k_0$. After identifying the cusp point, one can determine the nature of stability by identifying the sign of $Re(\omega_0)$. If $Re(\omega_0) = \omega_{0r} > 0$, the flow is absolutely unstable, and if $\omega_{0r} < 0$, the system is convectively unstable, provided that in both scenarios, the system is already temporally unstable. In the case of Fig. 3, we see that $\omega_{0r} = 0.043 > 0$, so that this does, indeed, correspond to a cusp point.

When the contour lines are deformed, a branch point arises up in the ω-plane, which is called a cusp point. At the same time, a pinch point appears in the k-plane. Further deformations of contour lines after forming the pinch point lead to a violation of causality, and these deformations are stopped. To determine if the cusp point has been

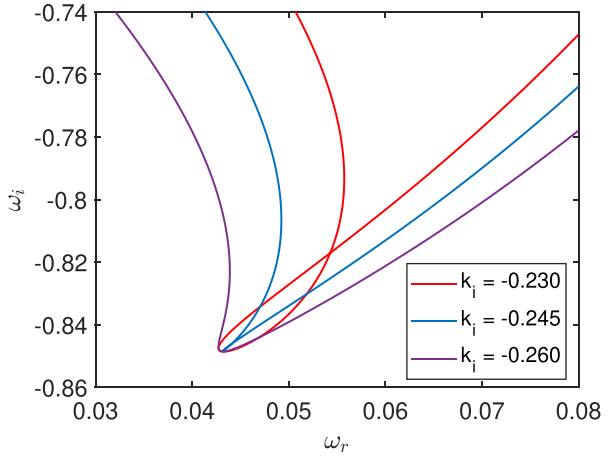

FIG. 3. Horizontal rays within the unstable wavenumber domain (i.e., lines of constant k_i) are mapped onto the complex frequency plane. The images intersect, and a singularity (identified by the angle doubling property of a local mapping) in the form of a cusp appears for a specific value of k_i. Here, $We = 2$ and $\rho = 0.01$, $\rho^G = 0.001$, $\sigma = 1$, $x = 0$, and $\chi = 0.3$.

formed by the continuous analysis of k-branches creating from two different halves of k-plane or not, the following procedure can be followed. According to Kupfer *et al.*,[34] one can check that the cusp point is a pinch point by drawing a straight ray parallel to ω_r-axis from the cusp point to the image of the first contour line (for $k_i = 0$) and then counting the number of points that this ray intersects with the image of the first contour line. If the number of intersections between this ray and the image of the first contour line is odd, then this cusp point has been formed by two k-branches creating from two different halves of k-plane and the cusp point are named as a pinch point.[34,39–41]

The procedure was applied to liquid jets in Alhushaybari[42] and Alhushaybari and Uddin[43] for the case of viscoelastic liquid jets. In general, for liquid jets, the critical parameter that influences the transitions between convective to absolute instability is the dimensionless Weber number. In order to determine the critical Weber number, We_c, for a given set of parameter values, we first fix a value of the Weber number and use the cusp map method (typically small values of the Weber number produce a cusp as outlined earlier, and this is then checked to ensure it does correspond to absolute instability with particular attention paid to where the cusp is located in the complex ω-plane). Absolute instability only occurs when $\omega_r > 0$. This procedure is then repeated with increments to the Weber number until ω_r is negative, in which case the process is terminated and the current value of the Weber number is labeled as the critical Weber number We_c. In Fig. 4, we show this methodology in action with the three values of the Weber number. As the Weber number is increased (here from $We = 1$ to $We = 3.4$), we see that the cusp moves in the complex frequency plane and, in particular, moves to the left, so that at $We = 3.4$, the cusp is now located at $\omega_r = 0$. Further increases in We will lead to no cusp formation or the presence of a cusp with $\omega_r < 0$. This procedure was used in Alhushaybari and Uddin[43] and Alhushaybari and Uddin.[44] This critical Weber number will mark the convective/absolute instability boundary (CAIB) between the convective and absolute regions and as stated by Montanero and Gana-Calvo;[6] this may be used as a good indication to identify between jetting and dripping of a liquid jet.

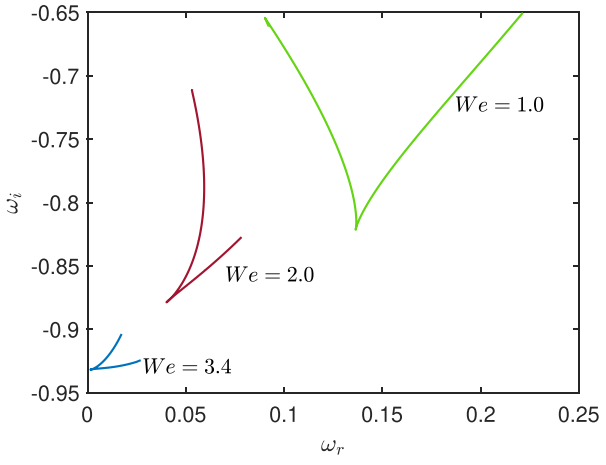

FIG. 4. The location of the cusp in the complex ω-plane for various values of the Weber number, $We = 1.0$ ($k_i = -0.208$), $We = 2.0$ ($k_i = -0.167$), and $We = 3.4$ ($k_i = -0.067$). Other parameters are $\rho = 0.01$, $\rho^G = 0.001$, $\sigma = 0.5$, $x = 0$, and $\chi = 0.5$. As the value of the Weber number is increased, the cusp moves toward the line $\omega_r = 0$.

VI. RESULTS AND DISCUSSION

In Fig. 5, we plot We_c against the surface tension ratio between the inner and outer fluids, σ, for the case of zero gravity, i.e., $Fr = \infty$, and for the case with gravity, $Fr = 1$. These curves effectively demarcate the parameter space where a compound jet is convectively unstable (regions above the curves) with regions where the jet is absolutely unstable (regions below). It should be noted in Fig. 5 that, in the zero gravity case, the critical Weber number decreases sharply with σ for small σ. Moreover, the effect of including gravity is to lead to a significant reduction in the value of the critical Weber number (which is always smaller than the zero gravity case). We can compare our results favorably with Vadivakkurasan[31] for a similar plot of the critical Weber number and its behavior with σ for the zero gravity case, although we note that in that work,[31] the author considers, in effect, an annular jet where inner jet/core is a quiescent gas, which differs from our case. Changes to the inner-to-outer jet radii ratio are important for different industrial applications with the configuration of small χ suitable for capsule and compound droplet formation, whereas larger values of χ are more suited to fiber production. Additionally, in taking the limit $\sigma \to 0$ with $\rho = 1$, our dispersion relation reduces to that of the single inviscid liquid jet with a surrounding gas. This was first investigated by Leib and Goldstein[27,28] who determined that the critical Weber in the case of $\rho^G = 0$ was given by $We_c = 3.14$ (see also Lin[3]). We find, using the aforementioned methodology, and in the limit described (i.e., the limiting case of a single jet), that the critical Weber number agrees with this value of 3.14. We note that the critical value of the Weber number, even for small values of σ, is not affected by the transitions in the most unstable wavenumber, k^*, from temporal analysis, which is explained in Sec. IV. In Fig. 6, we see that typically the critical Weber number, We_c, increases with χ although the changes are not significant (and do appear to *decrease* with χ for small χ). This behavior is seen for both the zero gravity case as well as the case with gravity. Finally, in Fig. 7, we plot the effect of changing the density ratio ρ on the critical Weber number, and we find that for

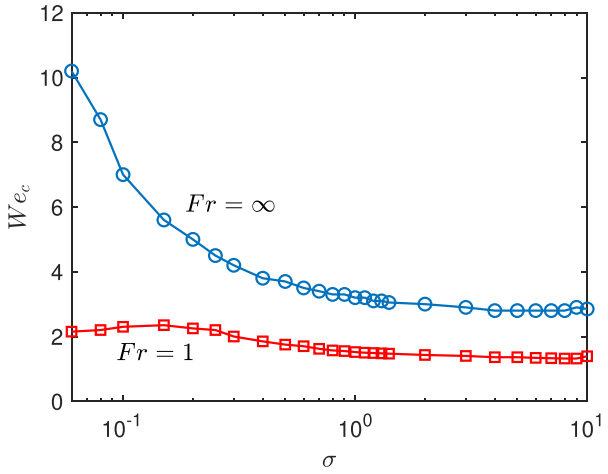

FIG. 5. The critical Weber number, We_c, plotted against the surface tension ratio σ. Here, the parameters are $\rho = 0.01$, $\rho^G = 0.001$, $x = 1$, and $\chi = 0.5$.

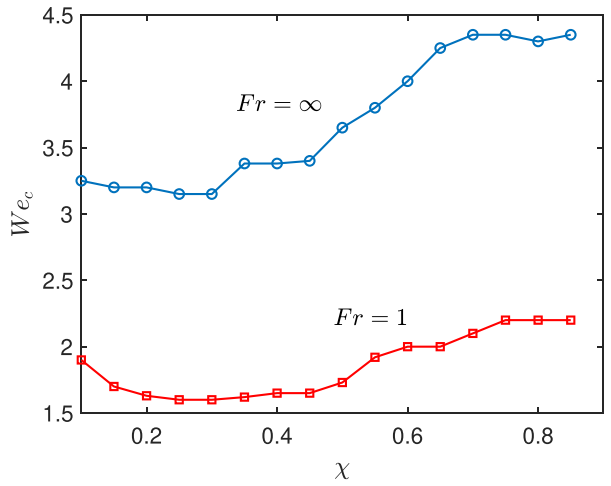

FIG. 6. The critical Weber number, We_c, plotted against the inner to outer radii ratio χ. Here, the parameters are $\rho = 0.01$, $\rho^G = 0.001$, $x = 1$, and $\sigma = 0.5$.

$0.01 < \rho < 0.5$, the critical Weber is fairly consistent in value and then decreases for $0.5 < \rho < 1$ and thereafter increases slightly.

VII. CONCLUSION

In this paper, we have considered the governing equations for an inviscid compound liquid jet, which is falling under gravity in the presence of a surrounding gas, which is subject to small linear disturbances. Using a linear stability analysis and the resulting dispersion relation, we make use of the cusp map method developed by Kupfer[34] to investigate the convective-to-absolute instability boundary with regard to the critical Weber number under various parameter regimes. In particular, we have shown that the presence of gravity tends to reduce the critical Weber number for a range of different inner-to-outer fluid surface tension ratios, inner-to-outer radii ratio as well as density ratios. Moreover, we have shown that the critical Weber number typically decreases with surface tension ratio and increases with the inner-to-outer radii. These results help in understanding the instabilities of compound liquid jets with a view to appreciating the transition between dripping and jetting with the multitude of applications in engineering where such transitions are important. A possible extension, with some modifications, of this work is the breakup of a jet of molten nuclear core (corium) in a coolant, where according to Ref. 45, the regime is well within the absolute instability range. This and other such applications are the subject of current work by the authors.

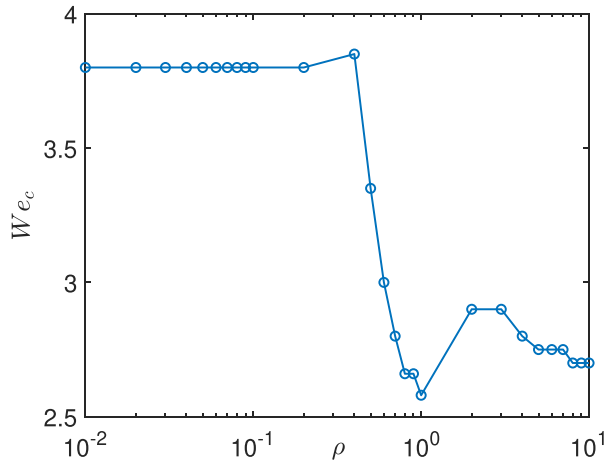

FIG. 7. The critical Weber number, We_c, plotted against the inner to outer density ratio ρ. Here, the parameters are $\sigma = 0.4$, $\rho^G = 0.001$, $Fr = \infty$, and $\chi = 0.5$.

AUTHOR DECLARATIONS

Conflict of Interest

The authors have no conflicts to disclose.

Author Contributions

Muhammad Faheem Afzaal: Data curation (equal); Investigation (equal). **Jamal Uddin:** Conceptualization (lead); Project administration (lead).

DATA AVAILABILITY

The data that support the findings of this study are available from the corresponding author upon reasonable request.

REFERENCES

[1]W. S. Rayleigh, "On the instability of jets," Proc. London Math. Soc. **s1-10**, 4 (1878).
[2]F. Savart, "Mémoire sur la constitution des veines liquides lancées par des orifices circulaires en mince paroi," Ann. Chim. **53**, 337 (1833).
[3]S. P. Lin, *Breakup of Liquid Sheets and Jets* (Cambridge University Press, Cambridge, 2003).
[4]J. Eggers, "Nonlinear dynamics and breakup of free surface flows," Rev. Mod. Phys. **69**, 865 (1997).
[5]J. Eggers and E. Villermaux, "Physics of liquid jets," Rep. Prog. Phys. **71**, 036601 (2008).
[6]J. M. Montanero and A. M. Gana-Calvo, "Dripping, jetting and tip streaming," Rep. Prog. Phys. **83**, 097001 (2020).
[7]K. S. Jayaprakash and A. K. Sen, "Droplet encapsulation of particles in different regimes and sorting of particle-encapsulating-droplets from empty droplets," Biomicrofluidics **13**(3), 034108 (2019).
[8]X. Liu, Y. Yu, D. Liu, J. Li, J. Sun, Q. Wei, Y. Zhao, S. J. Pandol, and L. Li, "Porous microcapsules encapsulating β cells generated by microfluidic electrospray technology for diabetes treatment," NPG Asia Mater. **14**, 39 (2022).
[9]M. Mishra, *Handbook of Encapsulation and Controlled Release* (CRC Press, 2015).
[10]C. H. Hertz and B. Hermanrud, "A liquid compound jet," J. Fluid Mech. **131**, 271—287 (1983).
[11]A. Sanz and J. Meseguer, "One-dimensional linear analysis of the compound jet," J. Fluid Mech. **159**, 55 (1985).
[12]S. Radev and B. Tchavadorov, "Linear capillary instability of compound jets," Int. J. Multiphase Flow **14**, 67 (1988).
[13]V. Ya. Shkadov and G. M. Sisoev, "Instability of a two layer capillary jet," Int. J. Multiphase Flow **22**, 363–377 (1996).
[14]A. Chauhan, C. Maldarelli, D. Papageorgiou, and D. S. Rumschitzki, "Temporal instability of compound threads and jets," J. Fluid Mech. **420**, 1–25 (2000).
[15]R. Qiao, K. Mu, X. Luo, and T. Si, "Instability and energy budget analysis of viscous coaxial jets under a radial thermal field," Phys. Fluids **32**, 122103 (2020).
[16]J. Uddin and S. P. Decent, "Breakup of inviscid compound liquid jets falling under gravity," J. Phys. A: Math. Theor. **43**, 485501 (2010).
[17]A. C. Ruo, F. Chen, and M. H. Chang, "Linear instability of compound jets with nonaxisymmetric disturbances," Phys. Fluids **21**, 012101 (2009).
[18]R. Suryo, P. Doshi, and O. A. Basaran, "Nonlinear dynamics and breakup of compound jets," Phys. Fluids **18**, 082107 (2006).

[19]G. Amini, M. Ihme, and A. Dolatabadi, "Effect of gravity on capillary instability of liquid jets," Phys. Rev. E **87**, 053017 (2013).
[20]T. V. Vu, S. Homma, J. C. Wells, H. Takakura, and G. Tryggvason, "Numerical simulation of formation and breakup of a three-fluid compound jet," J. Fluid Sci. Technol. **6**, 252–263 (2011).
[21]T. V. Vu, H. Takakura, J. C. Wells, and T. Minemoto, "Pattern formation of hollow drops from final breakup of a hollow jet," J. Fluid Sci. Technol. **6(6)**, 823–837 (2011).
[22]M. Mohsin, J. Uddin, S. P. Decent, and M. F. Afzaal, "Temporal instability analysis of inviscid compound jets falling under gravity," Phys. Fluids **25**, 012103 (2013).
[23]M. F. Afzaal, "Breakup and instability analysis of compound liquid jets," Ph.D. thesis (University of Birmingham, 2014).
[24]M. F. Afzaal, J. Uddin, M. A. Alsharif, and M. Mohsin, "Temporal and spatial instability of a compound jet in a surrounding gas," Phys. Fluids **27**, 044106 (2015).
[25]M. F. Afzaal and J. Uddin, "Nonaxisymmetric disturbances in compound liquid jets falling under gravity," Phys. Rev. E **94**, 043114 (2016).
[26]J. B. Keller, S. I. Rubinow, and Y. O. Tu, "Spatial instability of a jet," Phys. Fluids **16**, 2052 (1973).
[27]S. J. Leib and M. E. Goldstein, "The generation of capillary instabilities on a liquid jet," J. Fluid Mech. **168**, 479 (1986).
[28]S. J. Leib and M. E. Goldstein, "Convective and absolute instability of a viscous liquid jet," Phys. Fluids **29**, 952 (1986).
[29]S. P. Lin and Z. W. Lian, "Absolute instability of a liquid jet in a gas," Phys. Fluids **1**, 490 (1989).
[30]A. Chauhan, C. Maldarelli, D. T. Papageorgiou, and D. S. Rumschitzki, "The absolute instability of an inviscid compound jet," J. Fluid Mech. **549**, 81 (2006).
[31]M. Vadivukkarasan, "Transition from absolute to convective instability in a compound jet," Eur. J. Mech. B. Fluids **84**, 186–192 (2020).
[32]A. S. Utada, A. Fernandez-Nieves, J. M. Gordillo, and D. A. Weitz, "Absolute instability of a liquid jet in a coflowing stream," Phys. Rev. Lett. **100**, 014502 (2008).
[33]D. Runze, F. Ziwei, Z. Xiaolei, F. Qinfei, Y. Hua, W. Jin, and L. Liansheng, "Effect of drainage device on the transition of dripping to jetting modes," Phys. Fluids **35**, 053310 (2023).
[34]K. Kupfer, A. Bers, and A. K. Ram, "The cusp map method in the complex-frequency plane for absolute instabilities," Phys. Fluids **30**, 3075 (1987).
[35]P. G. Drazin, *Introduction to Hydrodynamic Stability* (Cambridge University Press, 1981).
[36]F. Charru, *Hydrodynamic Instabilities* (Cambridge University Press, 2011).
[37]R. Patne and V. Shankar, "Absolute and convective instabilities in combined Couette-Poiseulle flow past a neo-Hookean solid," Phys. Fluids **29**, 124104 (2017).
[38]P. K. Ray and T. A. Zaki, "Absolute/convective instability of planar viscoelastic jets," Phys. Fluids **27**, 014110 (2015).
[39]C. Camporeale, R. Vesipa, and L. Ridolfi, "Convective-absolute nature of ripple instabilities on ice and icicles," Phys. Rev. Fluids **2**, 053904 (2017).
[40]D. Bansal, T. Chauhan, and S. Sircar, "Spatiotemporal linear stability of viscoelastic Saffman-Taylor flows," Phys. Fluids **34**, 104105 (2022).
[41]D. Bansal, T. Chauhan, and S. Sircar, "Spatiotemporal linear stability of viscoelastic free shear flows: Nonaffine response regimes," Phys. Fluids **33**, 054106 (2021).
[42]A. Alhushaybari, "Convective and absolute instability of viscoelastic liquid jets," Ph.D. thesis (University of Birmingham, 2020).
[43]A. Alhushaybari and J. Uddin, "Convective and absolute instability of viscoelastic liquid jets in the presence of gravity," Phys. Fluids **31**, 044106 (2019).
[44]A. Alhushaybari and J. Uddin, "Absolute instability of free-falling viscoelastic liquid jets with surfactants," Phys. Fluids **32**, 013102 (2020).
[45]D. S. Pillai, P. Narayanan, S. Pushpavanam, T. Sundararajan, A. J. Sudha, and P. Chellapandi, "A nonlinear analysis of the effect of heat transfer on capillary jet instability," Phys. Fluids **24**, 12106 (2012).